Yagi-Configured Electrically Small Antenna with Quad-Polarization Diversity

Ming-Chun Tang[1*], and Qingli Lin[1]
[1] School of Microelectronics and Communication Engineering
Chongqing University
Chongqing, China
tangmingchun@cqu.edu.cn, 201812131045@cqu.edu.cn

Richard W. Ziolkowski[2]
[2] Global Big Data Technologies Centre
University of Technology Sydney
Ultimo NSW 2007, Australia
richard.ziolkowski@uts.edu.au

***Abstract* — A polarization-reconfigurable, high-directivity, Yagi-configured, near-field resonant parasitic (NFRP), electrically small antenna (ESA) is presented. The antenna is composed of a director, a reflector, and an electrically-controlled driven element loaded with four p-i-n (PIN) diodes. Two linear polarization (*x*-LP and *y*-LP) and two circular polarization (LHCP and RHCP) states are achieved simply by controlling the ON/OFF states of the PIN diodes. The measured results demonstrate that in its *x* (*y*)-LP state, the peak realized gain, front-to-back ratio, and radiation efficiency values are, respectively, ~3.08 (3.2) dBi, ~11.0 (11.05) dB, and ~77% (73%), and that in its LHCP (RHCP) state they are, respectively, ~3.0 (3.1) dBi, ~ 12.1 (11.18) dB, and ~ 72% (70%).**

Keywords—electrically small antennas; near-field resonant parasitic elements; polarization-reconfigurable antennas; Yagi-configured antennas.

I. Introduction

Yagi-Uda antennas [1] with their high directivity, simple configuration, and low cost have been developed for many applications [2]. As wireless communication systems have evolved, the room available on mobile platform for their antenna systems has become more and more limited. Several types of Yagi-configured electrically small antennas (ESAs) have been introduced to accommodate these space-limited platforms [3], [4]. Multi-functional and reconfigurable antennas have been studied extensively to meet these needs. However, only a few polarization-reconfigurable Yagi-based systems have been investigated. Integrating polarization reconfigurability with a Yagi-configured ESA could provide many advantages for space-limited wireless applications.

A polarization-reconfigurable, Yagi-configured ESA with quad-polarization diversity is presented in this paper. The antenna is composed of a director, a reflector and an electrically-controlled driven element integrated with four PIN diodes. By controlling their ON/OFF states, the antenna can achieve four different polarization states, i.e., *x*-LP , *y*-LP, LHCP, and RHCP. The electrically small size of the overall system, $ka = 0.7$, with its four polarization diverse states and excellent end-fire radiation performance characteristics makes it a very attractive candidate in space-limited wireless applications.

II. Antenna Design

Fig. 1 illustrates the developed Yagi-configured polarization-reconfigurable ESA. The antenna consists of three substrate layers. They are labeled as Layer_1, Layer_2 and Layer_3, respectively. All three substrates are Rogers 6010 with relative dielectric constant $\varepsilon_r = 10.2$, loss tangent $\tan\delta = 0.0023$, and copper cladding thickness 0.018 mm. The director and reflector are printed on the upper surface of Layer_1 and Layer_3 respectively. The middle layer, Layer_2, supports the driven element, which is printed on its lower surface. The antenna is differentially-fed by two parallel strips. One is connected to the center conductor of the coax, the other is connected to its outer conductor. The specific size and polarization states of the ESA are listed in Table I and Table II, respectively.

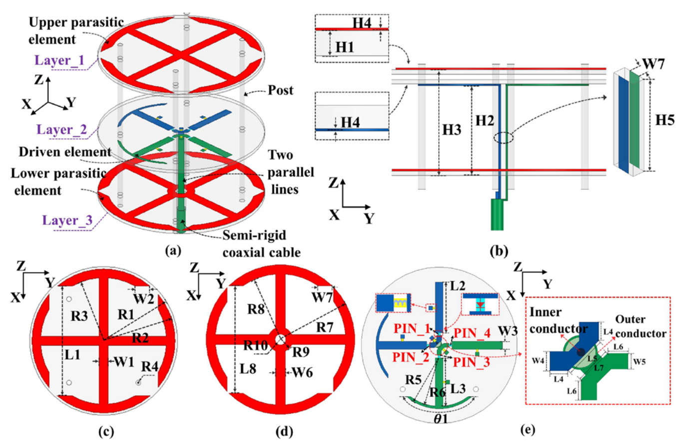

Fig. 1 Configuration and design parameters of the polarization-reconfigurable Yagi-configured ESA. (a) 3-D isometric view. (b) Side view. Upper surfaces of (c) Layer_1 and (d) Layer_3. (e) Lower surface of Layer_2.

TABLE I
Optimized Design Parameters of the Polarization-Reconfigurable ESA (dimensions in millimeters)

R1=32	*R2=31*	*R3=27.3*	*R4=1.05*	*R5=20.5*
R6=19.5	*R7=31.9*	*R8=28*	*R9=5.32*	*R10=2.32*
L1=47.2	*L2=24.3*	*L3=24*	*L4=1.89*	*L5=4.4*
L6=2	*L7=3.85*	*L8=45.4*	*W1=3.9*	*W2=6.37*

W3=3.2	*W4=2*	*W5=1.6*	*W6=4*	*W7=2.4*
W8=3.5	*θ=60°*	*H1=1.27*	*H2=26.27*	*H3=30.41*
H4=0.018	*H5=33*	*Null*		

TABLE II
THE PIN DIODE STATES TO ATTAIN THE FOUR POLARIZATION STATES

State	*PIN_1*	*PIN_2*	*PIN_3*	*PIN_4*
x-LP	*ON*	*OFF*	*ON*	*OFF*
y-LP	*OFF*	*ON*	*OFF*	*ON*
LHCP	*ON*	*OFF*	*ON*	*ON*
RHCP	*ON*	*ON*	*OFF*	*ON*

III. SIMULATED AND MEASURED RESULTS

The optimized polarization-reconfigurable Yagi-configured ESA shown in Fig. 1 was fabricated, assembled, and measured. The fabricated prototype is shown in Fig. 2.

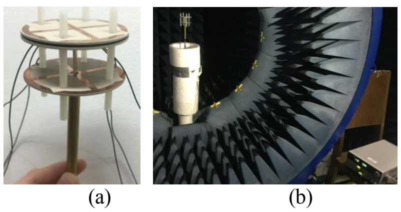

Fig. 2 Fabricated polarization-reconfigurable antenna. (a) 3-D isometric view. (b) Antenna under test (AUT) in the anechoic chamber.

The simulated and measured $|S_{11}|$ curves are shown in Fig. 3 for the *x*-LP, *y*-LP, LHCP, and RHCP states of the prototype. The simulated (measured) –10-dB impedance bandwidths of the *x*- and *y*- LP states are, respectively, from 0.941 to 0.987 GHz (0.945 to 0.976 GHz) and from 0.942 to 0.986 GHz (0.946 to 0.972 GHz). The simulated (measured) –10-dB impedance bandwidths of the LHCP and RHCP states are, respectively, from 0.937 to 0.995 GHz (0.934 to 0.986 GHz) and from 0.934 to 0.986 GHz (0.936 to 0.97 GHz).

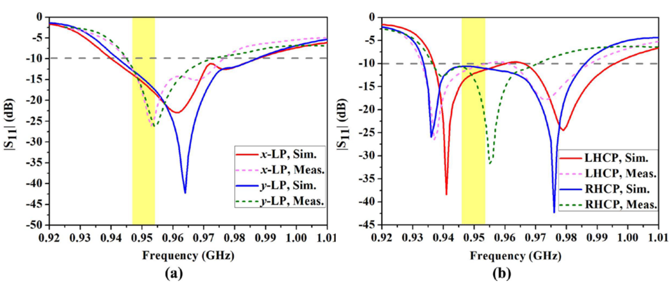

Fig. 3 Simulated and measured $|S_{11}|$ values of the polarization-reconfigurable ESA. (a) Two LP states. (b) Two CP states. (The measured overlapping bandwidth is highlighted by the yellow region.)

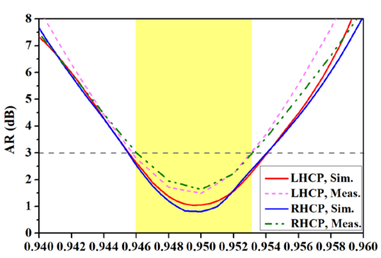

Fig. 4 Simulated and measured AR values of the polarization-reconfigurable ESA. (The measured overlapping bandwidth is highlighted by the yellow region.)

The simulated and measured AR values of the two CP states are plotted in Fig. 4. The simulated (measured) 3-dB bandwidths of the LHCP and RHCP states are the same from 0.946 to 0.954 GHz (0.946 to 0.953 GHz). Considering both the –10-dB impedance bandwidth and the 3-dB AR bandwidth, the measured overlapping operational bandwidth covered 7.0 MHz from 0.946 to 0.953 GHz for all four polarization reconfigurable states.

The simulated and measured normalized realized gain patterns of the four states at the selected operational frequency, 0.95 GHz, are plotted in Figs. 5 (a)-(d), respectively. In particular, the simulated (measured) peak realized gain, FTBR, and radiation efficiency (RE) values in the *x*-LP state are 3.8 (3.08) dBi, 10.93 (11.0) dB, and 87.9% (77%), respectively. The corresponding values in the *y*-LP state are 4.2 (3.2) dBi, 11.34 (11.05) dB, and 86% (73%), respectively. The simulated (measured) peak realized gain, FTBR, and RE values in the LHCP state are 3.8 (3.0) dBi, 14.39 (12.1) dB, and 82% (72%), respectively. The corresponding values in the RHCP state are 3.8(3.1) dBi, 14.72 (11.18) dB, and 82% (70%), respectively.

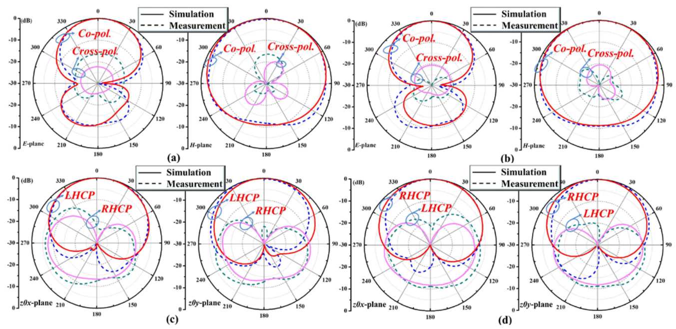

Fig. 5 The simulated and measured normalized realized gain patterns of the prototype operating at 0.95 GHz for all of its four polarization states. (a) *x*-LP state. (b) *y*-LP state. (c) LHCP state. (d) RHCP state.

IV. CONCLUSION

A polarization-reconfigurable Yagi-configured ESA was presented in this paper. The antenna realizes the transition between its *x*-LP, *y*-LP, LHCP, and RHCP states by controlling the ON/OFF state of four PIN diodes. The measured overlapping bandwidth between the –10-dB impedance bandwidth and 3-dB AR bandwidth for all four polarization states was 7 MHz, from 0.946 to 0.953 GHz. The demonstrated performance characteristics of its electrically small design make it attractive for the next-generation of narrowband wireless applications, e.g., WiFi, V2V, and D2D connectivity.

REFERENCES

[1] H. Yagi, "Beam transmission of ultra-short waves," *Proc. Inst. Radio Eng.*, vol. 16, no. 6, pp. 715–740, Jun. 1928.

[2] M. Nasir, Y. Xia, M. Jiang, and Q. Zhu, "A novel integrated Yagi–Uda and dielectric rod antenna with low sidelobe level," *IEEE Trans. Antennas Propag.*, vol. 67, no. 4, pp. 2751-2756, Apr 2019.

[3] M.-C. Tang and R. W. Ziolkowski, "Efficient, high directivity, large front-to-back-ratio, electrically small, near-field-resonant-parasitic antenna," *IEEE Access.*, vol. 1, pp. 16-28, 2013.

[4] M.-C. Tang, R. W. Ziolkowski, S. Xiao, and M. Li, "A high-directivity, wideband, efficient, electrically small antenna system," *IEEE Trans. Antennas Propag.*, vol. 62, no. 12, pp. 6541-6547, Dec. 2014.